INFLUENCE OF VEHICLE RELATED HEATS ON 'BLACK ICE'

Akihiro FUJIMOTO*, Hiroshi WATANABE* and Teruyuki FUKUHARA*
** University of Fukui, 3-9-1*
Bunkyo Fukui-city, 910-8507, Japan
afujimot@u-fukui.ac.jp

ABSTRACT

Melting of the snow and ice (S/I) on a road and the subsequent refreezing often cause traffic accidents. These phase changes tend to occur after traffic jam below the freezing point and is changeable to 'black ice'. However, the consideration about the relation between the vehicle related heats (vehicle heats) and 'black ice' has been inadequate.

There are many road freezing forecasting (RFF) models, but most of them have not given careful consideration to the thermal influence of vehicles on the S/I conditions. We have developed an extended RFF model in consideration of three kinds of vehicle heats, i.e. tire frictional heat, vehicle radiant heat and sensible heat due to vehicle passage and it is named vehicle heat RFF (VHRFF) model.

Numerical simulations using the VHRFF model were conducted to understand the influence of the vehicle heats on the S/I conditions associated with traffic stop and go at a traffic light.

The numerical results could show that the vehicle heats have the potential to melt and to freeze the S/I on a road surface, and inferred that the melting and refreezing eventually induce the formation of 'black ice' on the road.

1. INTRODUCTION

We have been developing a road freezing forecast (RFF) model using a heat balance method to reconcile the reduction of road management expenses and safe traffic in winter. The heat balance of the S/I on a road is determined by both internal and external thermal factors. The internal factors include the road structures, the thermal properties of pavement and the road foundation materials. The external factors consist of natural factors and artificial factors. The former are involved in weather and geographical features and the latter include road salts, heat from vehicles and mechanical snow removal.

RFF models based on the heat balance on the road surface have been reported by Sass [1], Shao & Lister [2], Ishikawa et al. [3] and Morstad [4], etc. The common feature of these models is that only the natural factors determine temperature of the road surface.

Following these studies, Ishikawa et al. [5] and Takahashi et al. [6] reported that radiant heat from the bottom of a vehicle (vehicle radiant heat) significantly affects the heat balance on the road surface. Kinoshita et al. [7] and Fujimoto et al. [8] pointed out that the tire frictional heat (heat transfer between tire and road surface) is important in the occurrence of 'black ice' on the road surface. Fujimoto et al. [9] reported that the sensible heat due to vehicles induced wind velocity (vehicle sensible heat) is an important factor for the heat balance of the road surface according to weather and traffic conditions. Moreover, Fujimoto et al. [10] reported that road surface temperature, T_{ps} (°C), fluctuates about the freezing point by vehicle stop and go behavior due to a traffic light.

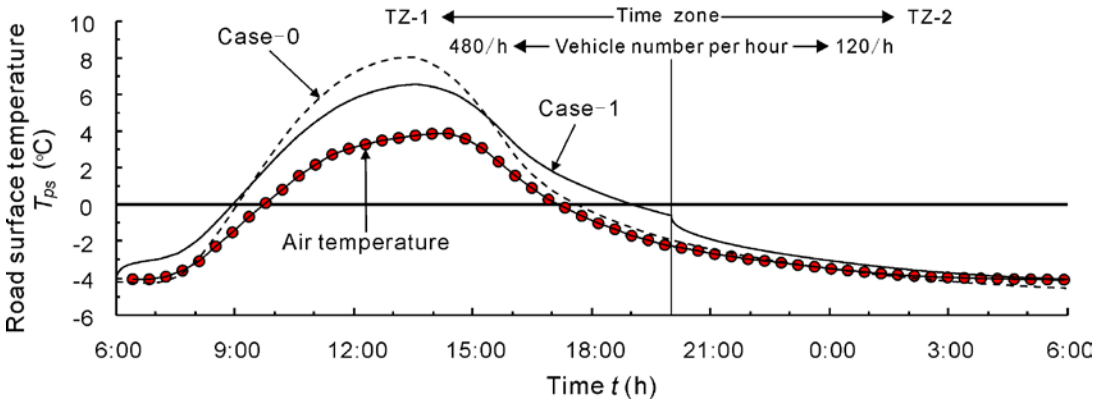

(a) Road without a traffic light (Case-1)

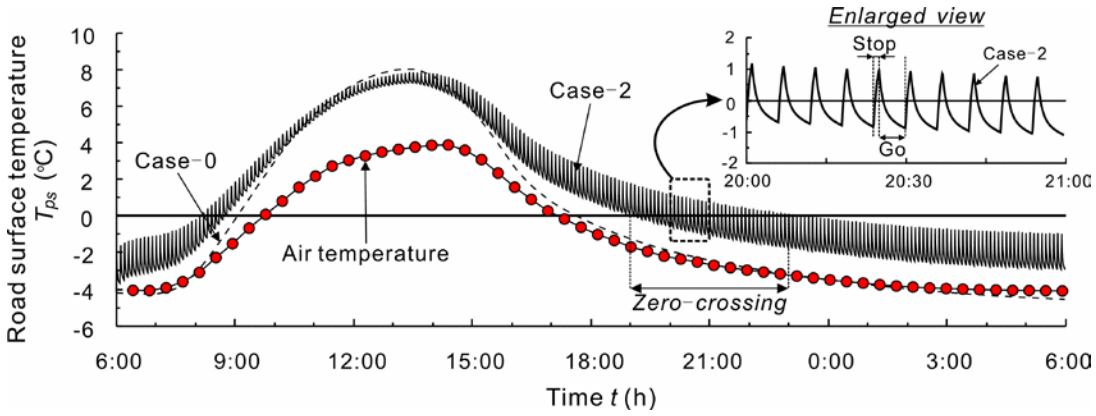

(b) Intersection (Case-2)

Figure 1. Diurnal variations of road surface temperature.

Figure 1 (a) and (b) show the diurnal variations of T_{ps}. In this figure, T_{ps} for three different traffic conditions were shown: Case-0: no vehicle, Case-1: traffic on a road without a traffic light, and Case-2: traffic at an intersection with a traffic light. The assumed vehicle stop and go time (duration) at the traffic light were 1 and 5 minutes, respectively throughout the day for Case-2. Comparing T_{ps} of Case-0 with that of Case-1, it is seen that the former is relatively high for the daytime and relatively low for the nighttime. The shade made by the vehicle body and the vehicle sensible heat lower T_{ps}, while the tire frictional heat and vehicle radiant heat contribute to the rise of T_{ps}.

T_{ps} of Case-2 is changed in wavelike fashion due to the difference in the vehicle heats between the vehicle stop and go time. T_{ps} rises during the vehicle stop time because of tire frictional heat, while T_{ps} falls during the vehicle go time. Tire frictional heat of 300 W/m^2 is intermittently supplied in the periods of 6:00-8:00 and 21:00-6:00 to the road surface, so that the amplitude of T_{ps} becomes 2°C. T_{ps} fluctuated about the freezing point at this phenomenon is called “zero-crossing” in this study. The “zero-crossing” was, however, found out by the simulation for a dry pavement. Therefore, the possibility of melting and refreezing of the S/I on a road surface is still uncertain.

From this research background, a new simulation using the VHRFF model was performed to quantitatively examine the correlation between the formation of ‘black ice’ on the road surface and vehicle stop and go behavior due to a traffic light.

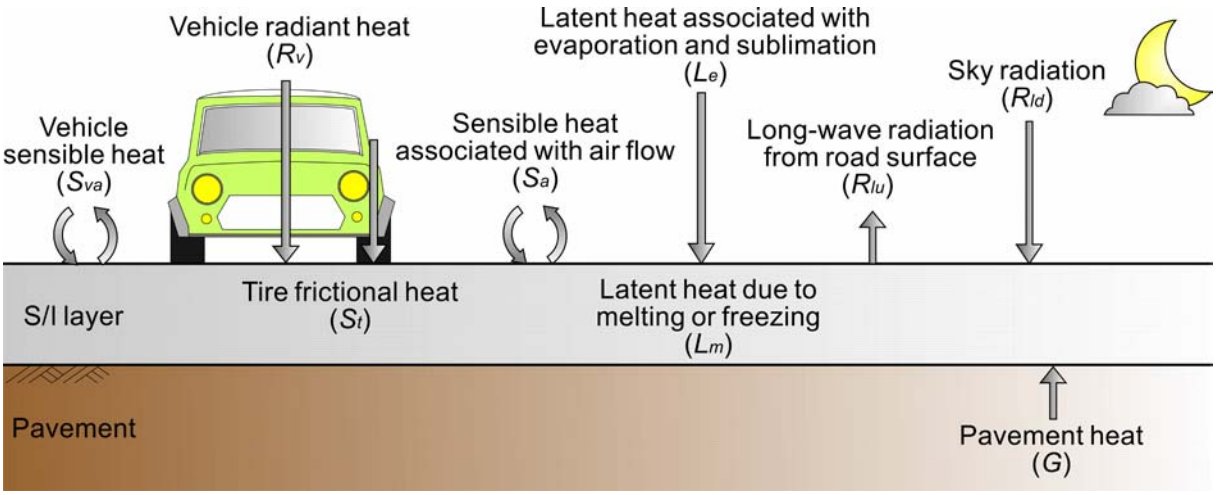

Figure 2. Schematic view of heat balance of S/I layer in night time.

2. HEAT AND MASS TRANSFER THEORY FOR SNOW/ICE ON ROAD

2.1 Heat Balance Equation

Figure 2 shows the heat balance of the S/I layer in the nighttime. The heat balance of the S/I layer in the vehicle passage part is given by Eq. (1):

$$(\rho c)_{si}\frac{\partial T_{si}}{\partial t}\Delta z_{si} = G + R_{ld} - R_{lu} + S_a + L_e + L_m + Q_v = Q_{net} \tag{1}$$

where $(\rho c)_{si}$ is the volumetric heat capacity of the S/I layer (J/m^{3}K), t is time (s), T_{si} is the temperature of the S/I layer (°C), Δz_{si} is the thickness of the S/I layer (m), G is the pavement heat flux (W/m^2), R_{ld} is the sky radiant heat flux (W/m^2), R_{lu} is the long-wave radiant heat flux from the S/I surface (W/m^2), S_a is the sensible heat flux associated with air flow (W/m^2), L_e is the latent heat flux associated with sublimation or condensation (W/m^2), L_e is the latent heat flux associated with melting or freezing of the S/I layer (W/m^2), Q_v is the total vehicle heat flux (W/m^2) expressed by Eq. (8) and Q_{net} is the net heat flux across the S/I layer. Since L_e is much smaller than other heat fluxes, L_e is disregarded in this paper.

(1) Pavement Heat

Heat flux across the pavement surface (pavement heat), C_{sp}, is calculated using a thermal resistance, R_c (m^{2}K/W), as follows:

$$C_{sp} = \frac{1}{\frac{\Delta z_{si}/2}{\lambda_{si}} + \frac{\Delta z_{ps}/2}{\lambda_p} + R_c}\left(T_{ps} - T_{si}\right) \tag{2}$$

where λ_{si} is the thermal conductivity of the S/I layer (W/mK), λ_p is the thermal conductivity of the pavement (W/mK), Δz_{ps} is the thickness of pavement surface layer (m), T_{ps} is the temperature of the pavement surface layer.

R_c depends on the volumetric air content, θ_a, of the S/I layer, which reflects the resistance of the heat flow path between the S/I and the pavement surface, and is given by Eq. (3), [11],

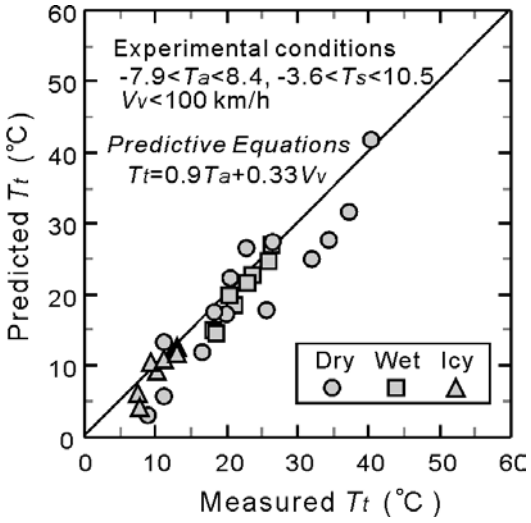

Figure 3. Correlation between predicted and measured tire temperatures.

$$R_c = 0.6 \times 10^{-3} \, exp(5.3\theta_a) \tag{3}$$

(2) Long-Wave Radiant Heat

R_{lu} is calculated by the Stefan-Boltzmann law,

$$R_{lu} = \varepsilon_{si}\sigma(T_{si} + 273.15)^4 \tag{4}$$

where ε_{si} is the emissivity of the S/I layer surface and σ is the Stefan-Boltzmann constant (5.67×10^{-8} W/m^{2}K^4). ε_{si} is expressed by the harmonic mean as follows:

$$\varepsilon_s = \varepsilon_i\theta_{si} + \varepsilon_w(1-\theta_{si}) \tag{5}$$

where ε_i is the emissivity of ice surface (= 0.98[12]), ε_w is the emissivity of water surface (= 0.96[12]), θ_{si} is the mass ice content.

R_{ld} is assumed to be constant of 270 W/m^2 in the present numerical simulations.

(3) Sensible Heat Flux Associated With Air Flow

S_a is evaluated using Newton's law of cooling,

$$S_a = \alpha_s(T_a - T_{si}) \tag{6}$$

where α_s is the heat transfer coefficient between the S/I layer surface and atmosphere (W/m^2/K) and T_a is an atmospheric temperature (°C). The value of α_s is estimated from the wind velocity, V_{ws} (m/s), using our previous experimental result, [13]:

$$\alpha_s = 6.4V_{ws}^{0.7} + 2.2 \tag{7}$$

(4) Vehicle Heats

The total vehicle heat flux, Q_v, is given by the sum of the tire frictional heat flux, S_t, the vehicle radiant heat flux, R_v, and the vehicle sensible heat flux, S_{va}. That is

$$Q_v = S_t + R_v + S_{va} \tag{8}$$

S_t may be calculated by Newton's law of cooling,

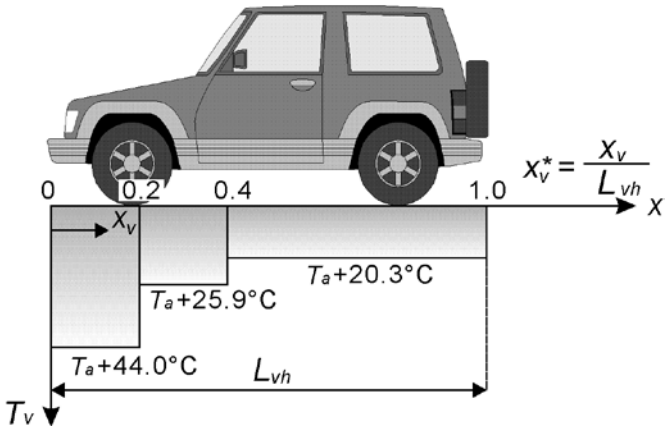

Figure 4. Spatial variation of temperature on bottom surface of vehicle in direction of vehicle movement.

$$S_t = \alpha_{tp}\left(T_t - T_{ps}\right) \tag{9}$$

where α_{tp} (=70 W/m^{2}K [8]) is the heat transfer coefficient between the S/I layer surface and tire, and T_t is a tire temperature (°C).

T_t is given by the following empirical correlation, regardless of road surface conditions (see Figure 3).

$$T_t = 0.9T_a + 0.33V_v \tag{10}$$

where V_v is vehicle speed (km/h).

R_v may be evaluated by the Stefan-Boltzmann law using the temperature, T_v, on the bottom surface of the vehicle. That is

$$R_v = \varepsilon_v \sigma\left(T_v + 273.15\right)^4 \tag{11}$$

where ε_v is the emissivity of the vehicle bottom (= 0.80).

The spatial variation of T_v in the direction of vehicle movement (x) is simplified as shown in Figure 4. That is

$$\begin{aligned} T_v &= T_a + 44.0 \quad \left(0 \le x_v^* \le 0.2\right) \\ T_v &= T_a + 25.9 \quad \left(0.2 \le x_v^* \le 0.4\right) \\ T_v &= T_a + 20.3 \quad \left(0.4 \le x_v^* \le 1.0\right) \end{aligned} \tag{12}$$

where x_v^* is the normalized distance (=x_v/L_{vh}, x_v: distance from the vehicle front, L_{vh}: vehicle length).

S_{va} is given by Newton's law of cooling as

$$S_{va} = \alpha_s\left(T_a - T_{ps}\right) \tag{13}$$

where α_s is the heat transfer coefficient (W/m^{2}K) and is expressed in terms of the vehicle induced wind velocity, V_w (m/s);

$$\alpha_s = 6.4V_w^{\,0.7} + 2.2 \tag{14}$$

Figure 5 shows the time variation of V_w for different vehicle speeds, V_v (km/hour). During acceleration

$$V_w = at \quad \left(0 \le t \le t_{v\,max}\right) \tag{15}$$

where $t_{v\,max}$ is elapsed time when V_w reaches a maximum, $V_{w\,max}$.

For the deceleration period

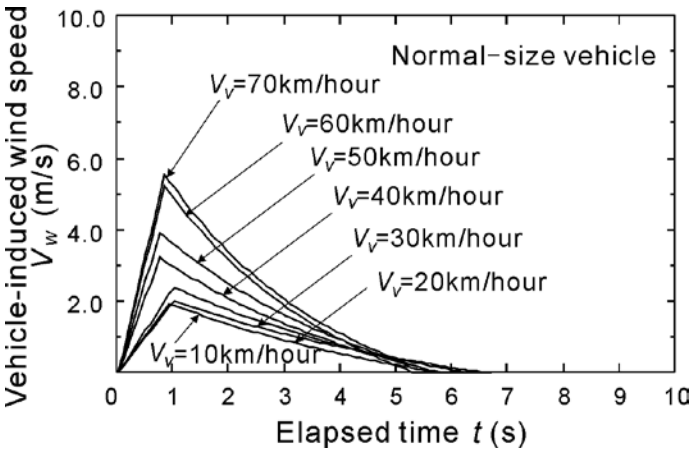

Figure 5. Time variation of vehicle-induced wind velocity for different vehicle speeds.

$$V_w = V_{w\,max}\, exp\{-b(t - t_{v\,max})\} - c(t - t_{v\,max}) \quad (t_{v\,max} \le t \le t_{v0}) \tag{16}$$

where t_{v0} is elapsed time when V_w becomes zero again. Coefficients, a, b, c, and the parameters, $V_{w\,max}$, $t_{v\,max}$ and t_{v0} in Eqs. (15) and (16) are given by the following functions of $V_{v,}$ respectively.

$$a = 0.08V_v \tag{17}$$

$$b = 0.28 \times 10^{-2} V_v + 0.13 \tag{18}$$

$$c = V_{w\,max}\, exp\{-b(t_{v0} - t_{v\,max})\}/(t_{v0} - t_{v\,max}) \tag{19}$$

$$V_{w\,max} = 0.08V_v \tag{20}$$

$$t_{v\,max} = 1.2 exp(-0.3 \times 10^{-2} V_v) \tag{21}$$

$$t_{v0} = -1.4 \times 10^{-2} V_v + 7.6 \tag{22}$$

2.2 Mass Balance Equation

The time change rate of the ice mass, M_i (kg/m^2), in the S/I layer is given by Eq. (23):

$$\frac{\partial M_i}{\partial t} = M_{if} + M_{il} - M_{iw} \tag{23}$$

where M_{if} is the snowfall mass flux (kg/m^{2}s), M_{il} is the phase change mass flux due to sublimation (kg/m^{2}s) and M_{iw} is the melting or freezing mass flux (kg/m^{2}s). Since the present aspect is put on the formation of 'black ice' associated with traffic stop and go at a traffic light, M_{if} and M_{il} are disregarded in this paper.

M_{iw} is given by Eq. (24).

$$M_{iw} = \frac{1}{1000}\frac{Q_{net}}{q_m} \tag{24}$$

where q_m is the heat of fusion (kJ/kg).

Table 1 Weather, traffic and initial snow conditions for numerical simulations.

Simulation period			
Night time (5 hours)			
Weather condition		Initial snow condition	
Air temperature	: -5°C	Thickness	: 5 mm
Relative humidity	: 95%	Density	: 800 kg/m^3
Wind velocity	: 0 m/s	Mass ice content	: 100%
Sky radiation	: 270 W/m^2	Temperature	: 0°C
Traffic condition			
Simulation	Traffic volume F_t	Vehicle speed V_V	Stop time t_{vs} / go time t_{vm}
Case-0	0	-	-
Case-1	200 vehicles/hour	30 km/hour	-
Case-2	200 vehicles/hour	30 km/hour	3 minutes / 5 minutes (0 – 2 hours: Ti-1) 10 seconds / 5 minutes (2 – 5 hours: Ti-2)

3. EFFECT OF VEHICLE HEATS AND TRAFFIC CONDITIONS ON S/I LAYER ON A ROAD

3.1 Model Assumptions

The following three assumptions were applied to the present numerical simulations.

i) The frequency of vehicle passage is constant and is calculated from hourly traffic volume.
ii) Vehicles all pass over the same track within a lane.
iii) All vehicles are the cars with a standard size (L_{vh} = 4.0 m).

3.2 Simulation Conditions

Three different simulation conditions were designed: Case-0: no vehicle, Case-1: a road without a traffic light, and Case-2: an intersection with a traffic light. The weather, traffic and initial snow conditions are shown in Table 1. The numerical simulations were carried out for 5 hours in the night. The time increment of the computation, Δt, was one second. It is assumed that an atmospheric temperature, T_a, is -5°C, the relative humidity, RH_a, is 95%, the wind velocity is 0 m/s and the sky radiation, R_{ld}, is 270 W/m^2. These values are also assumed to be constant for the whole simulation period. The snow was accumulated before traffic jam associated with going home. The initial snow condition on the road is given as follows: the snow height is 5 mm, the snow density is 800 kg/m^3 and the mass ice content is 100% (completely dry snow).

The traffic frequency, F_t (number of vehicles per hour), was assumed to be 200 for the computation period. The vehicle speed, V_v, was constant at 30 km/h for both Case-1 and Case-2. Regarding Case-2, the vehicle stop and go time at the traffic light, t_{vs} and t_{vm}, were set as 3 minutes and 5 minutes for the period from 0 to 2 hours (Ti-1), i.e. during traffic jam and then changed to 10 seconds and 5 minutes for the period from 2 to 5 hours (Ti-2), i.e. during non-traffic jam, respectively.

3.3 Simulation Results

(1) Heat Fluxes

Figure 6 shows the time variations of heat fluxes (R_v, S_{va}, L_m and R_{lu}+R_{ld}) for first 30 minutes of the simulation period for Case-2. S_a was almost zero and R_{lu} + R_{ld} was constant at 40 W/m^2. R_v of 340

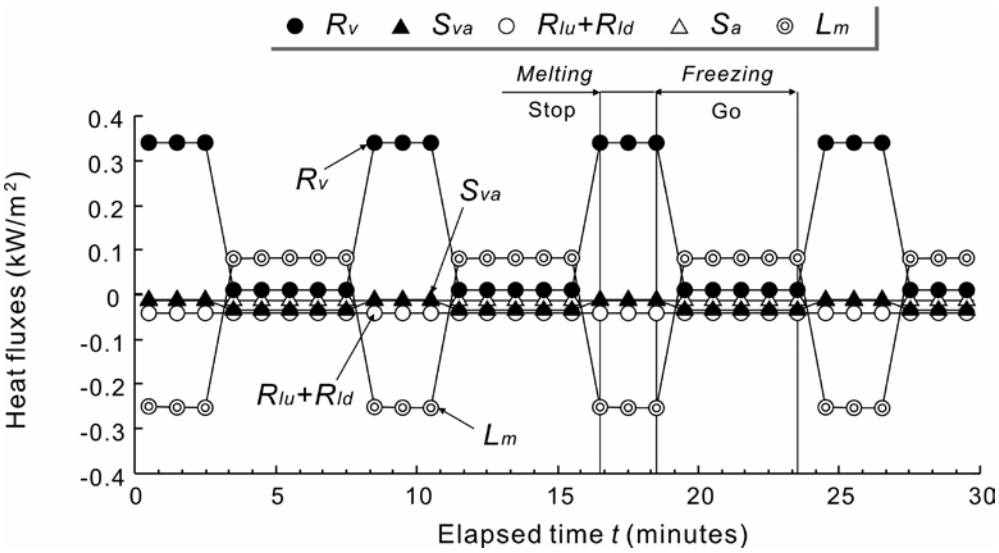

Figure 6. Time variations of heat fluxes across S/I layer (Case-2).

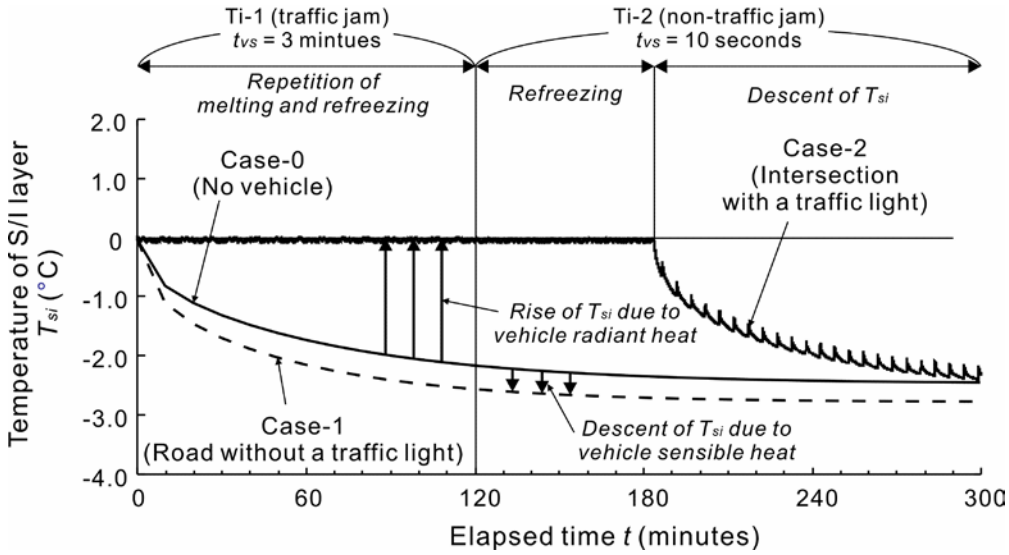

Figure 7. Time variations of temperature of S/I layer for three different traffic conditions.

W/m^2 was supplied to the S/I layer for the vehicle stop time and led to negative L_m associated with the melting of the S/I layer. L_m, however, changed from negative to positive, as soon as vehicles began to go. The positive L_m means the freezing of the S/I, i.e. the refreezing after the melting. The refreezing was attributed to the decrease in R_v and the occurrence of S_{va}.

(2) Temperature

Figure 7 shows the time variations of T_{si} for Case-0, Case-1 and Case-2, respectively. T_{si} of Case-0 falls with elapsed time due to negative R_{lu} and approaches the equilibrium temperature. Comparing T_{si} of Case-0 with that of Case-1, the latter was about 0.5°C lower than the former. This is caused by the vehicle radiant heat, S_{va}. As traffic frequency or the vehicle speed increases, the decent of T_{si} becomes obvious. On the other hand, T_{si} = 0°C continued for about one hour after the traffic jam had ended. After that, T_{si} of Case-2 started falling in wavelike fashion with time.

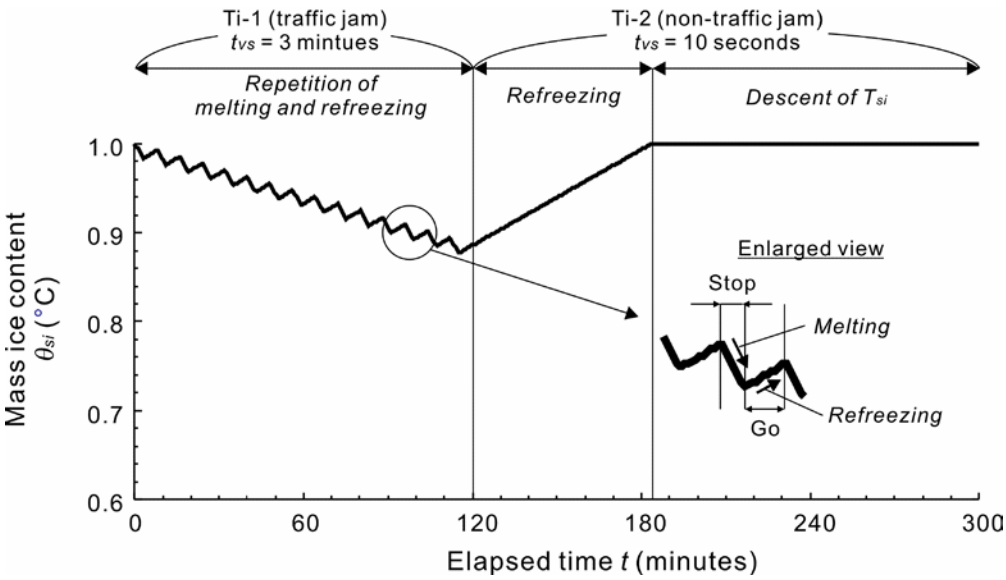

Figure 8. Time variation of mass ice content for Case-2.

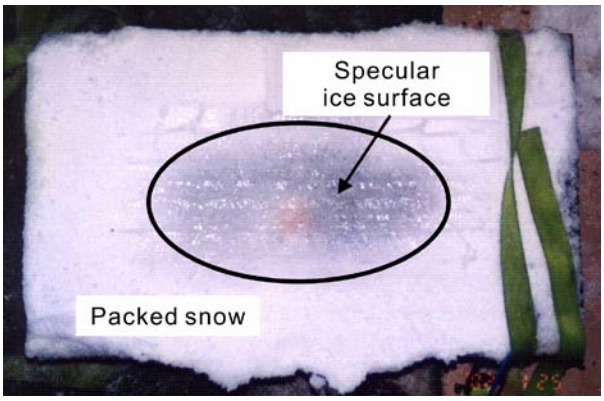

Photograph 1 Refreezing of packed snow surface after melting due to tire frictional heat associated with wheel slide. (number of passage of wheel = 5000, room air temperature = -3°C)

(3) Mass ice content

Figure 8 shows the time variation of the mass ice content, θ_{si}, of the S/I layer. Both values of θ_{si} for Case-0 and Case-1 were 1.0 for the simulation period (not shown in this Figure). There was no melting of the S/I layer for Case-0 and Case-1. θ_{si} of Case-2 varied in wavelike fashion due to the difference in the vehicle heats between the vehicle stop and go time. θ_{si} decreased due to snow melting during the vehicle stop time, while θ_{si} increased due to refreezing during the vehicle go time. The melting of the S/I layer excelled than the freezing during the traffic jam. Taking account of T_{si} = 0°C for Case-2 during the traffic jam, it is reasonable that the melting of the S/I layer is imperfect. However, after the traffic jam was over, the freezing of the S/I layer excelled than the melting and θ_{si} asymptotically approached 1 again. Consequently, the time rate of the refreezing was twice that of the melting. Since this refreezing process is quite similar to that observed in our wheel-tracking test [8], it is inferred that the S/I layer surface may become slipperier like ‘black ice’ or a specular ice surface (ice road surface) shown in Photograph 1.

4. CONCLUSIONS

Numerical simulations using the proposed VHRFF model were carried out to examine the correlation between the formation of 'black ice' on a road surface and vehicle stop and go time by a traffic light.

The numerical results could show that the vehicle heats have the potential to melt and freeze the snow and ice on a road surface, and inferred that the repetition of melting and freezing of the snow and ice eventually may induce the formation of 'black ice' on the road surface.

REFERENCES

[1] B.H. Sass. 1992. A numerical model for prediction road temperature and ice. *The Journal of Applied Meteorology*, 31, 1499-1506.

[2] J. Shao & P.J. Lister. 1996. An automated nowcasting model of road surface temperature and state for winter road maintenance. *The Journal of Applied Meteorology*, 35, 1352-1361.

[3] N. Ishikawa, R. Naruse & N. Maeno. 1987. HEAT balance characteristics of road snow, *Low temperature science. Ser. A, Physical Sciences*, 46, 151-162.

[4] Morstad, B., Adams, E.E., McKittrick, L.R. & Bristow, J.R. 2004. Thermal model for contaminated snow on pavement, *Proceedings of the Fifth International Conference on Snow Engineering*, 5, 33-38.

[5] N. Ishikawa, H. Narita & Y. Kajiya. 2000. Heat balance characteristics of snow melting on roads, *Proceedings of Cold Region Technology Conference*, 16, 382-388.

[6] N. Takahashi, M. Asano & N. Ishikawa. 2005. Developing a method to predict road surface icing conditions applying a heat balance method, *Proceedings of Cold Region Technology Conference*, 21, 201-208.

[7] S. Kinosita, E. Akitaya & K. Tanuma. 1970. Snow and ice on roads. II., *Low temperature science. Ser. A, Physical Sciences*, 28, 311-323.

[8] A. Fujimoto, H. Watanabe & T. Fukuhara. 2006. Effects of tire frictional heat on snow covered road surface, *Standing International Road Weather Conference*,13, 117-122.

[9] A. Fujimoto, H. Watanabe & T. Fukuhara. 2007. Modeling of vehicle heats and its influence on surface temperature of dry road, *Journal of Japan Society of Civil Engineers*, 63, 2, 202-213.

[10] A. Fujimoto, H. Watanabe & T. Fukuhara. 2008. Effects of vehicle heats on temperature on a dry road surface, *Standing International Road Weather Conference*, 14.

[11] A. Fujimoto, H. Watanabe & T. Fukuhara. 2007. Thermal contact resistance between snow/ice layer and pavement surface, *Journal of Japan Society of Civil Engineers*, 63, 1, 156-165.

[12] Y.A. Cengel. 1998. Heat transfer: A practical approach. *Tata Mc-Graw-Hill publishing company limited*, 968.

[13] A. Fujimoto, H. Watanabe, T. Fukuhara, T. Saito, M. Nemoto, S. Mochizuki & T. Kishii. 2006. Heat and water vapor transfer between atmosphere and pavement surface under dry, wet, ice plate and packed snow state, *Journal of Snow Engineering of Japan*, 22, 3, 14-22.